



# A long range piezoelectric rotary motor with continuous output: Design, analysis and experimental performance



Shupeng Wang, Weibin Rong\*, Lefeng Wang, Zhichao Pei, Lining Sun

State Key Laboratory of Robotics and System, Harbin Institute of Technology, Harbin, Heilongjiang, 150080, China

## ARTICLE INFO

### Article history:

Received 12 January 2017

Received in revised form 28 May 2017

Accepted 31 May 2017

Available online 4 June 2017

### Keywords:

Continuous motion

Rotary motor

Piezoelectric

Long range

## ABSTRACT

This study proposes a novel piezoelectric rotary motor which can output long range continuous motion. With the help of two piezo-stacks which are located at a 90° included angle, the motor can achieve circular motion trajectory of a cylindrical driving surface and the rotor can be driven by the cylindrical surface to deliver long range continuous rotary motion without pause. The structure and operational principle are introduced in detail. The stiffness of the flexure hinge system is theoretically calculated and the result is verified by finite element analysis. A prototype of the proposed motor is manufactured and a set of experimental system is established to investigate the performance of the prototype. The experimental results confirm that the motor prototype can output long range continuous rotary motion stably. With the driving frequency increasing, the angular velocity of the prototype increases gradually while the angular acceleration decreases gradually. The angular velocity can reach 221,321  $\mu\text{rad/s}$  when the driving frequency is 512 Hz. The maximum loading capacity is about 2.65 N and the maximum output torque is about 4.94 Nmm when the driving voltage and frequency are 150 V and 1 Hz. The return error of the prototype is about 608  $\mu\text{rad}$  during the forward stroke of 28,970  $\mu\text{rad}$  and the error percentage is about 2.1%. We can obtain a satisfactory angular velocity by choosing a proper frequency for the motor.

© 2017 Elsevier B.V. All rights reserved.

## 1. Introduction

With the development of micro/nano science and technology, the demand for precision/ultra-precision actuators has become increasingly urgent due to their wide applications in research and engineering fields such as microelectronics, microrobotics, biomedical science, aerospace technology, optics and genetic engineering [1–3]. Many smart materials have been used as precise actuators, including piezoelectric materials, shape memory alloys, magnetostrictive and electrostrictive materials [4–7]. Recent years, piezoelectric materials have gained extensive attentions from researchers all over the world due to their advantages of small size, high resolution, large output force, high stiffness, rapid responses and so on [8–12]. Many high-precision actuators that have been developed are driven by piezoelectric materials [13,14]. So far, the piezoelectric-driven actuator can be mainly classified as inchworm actuator [15–17], stick-slip actuator [18–24], ultrasonic actuator [25–30], and so on.

The inchworm type actuator usually consists of one feeding module and two clamping modules and it is a type of bionic actuator

imitating the movement of the inchworm in nature. The inchworm actuator can achieve nanometer resolution positioning over a long motion range. However, it needs at least three phases which cause its operation to be complex and the clamping operation and relatively large volume reduce its driving frequency [15–17]. The stick-slip type actuator is equipped with a friction element that can move forward slowly and backward rapidly. When the friction element moves forward slowly, the rotor/mover can be driven by the frictional force and when the friction element moves backward rapidly, the rotor/mover cannot follow the fast motion of the friction element and remains in place due to its inertia. Therefore, the rotor/mover can produce an unlimited displacement by continuously repeating these operations. The stick-slip actuator is rather simple made superior by its compact structure, simple operation, and accurate step capability compared with other types of actuators, but it has the drawback of small loading capacity due to its invariant normal force [18–24]. The ultrasonic type actuator is driven by the ultrasonic vibration excited at resonance. The stator can produce elliptical driving trajectory on the frictional contact surfaces by this vibration energy. A rotor/mover, placed against the stator, can be then driven by using the elliptical driving trajectory. The ultrasonic actuator possesses many merits, including lightweight, compact size, high speed and so on. Nevertheless, since the movement of an ultrasonic motor is generated through the fric-

\* Corresponding author.

E-mail address: [rwb@hit.edu.cn](mailto:rwb@hit.edu.cn) (W. Rong).

**Table 1**  
Performance of piezoelectric actuators.

Reference	Year	Type	Velocity	Output
[18]	2016	Ultrasonic	$1.65 \times 10^7 \mu\text{rad/s}$	53 Nmm
[31]	2016	Ultrasonic	$3.58 \times 10^7 \mu\text{rad/s}$	6.26 Nmm
[32]	2017	Stick-slip	$1165 \mu\text{rad/s}$	70.6 Nmm
[33]	2015	Stick-slip	$32000 \mu\text{rad/s}$	152.9 Nmm
[34]	2013	Inchworm	$6508.5 \mu\text{rad/s}$	93.1 Nmm
[35]	2014	Inchworm	$71300 \mu\text{rad/s}$	19.6 Nmm

tional coupling between the stator and the rotor/mover, wear and heat generation are inevitable problems [25–30]. Table 1 summarizes the performance data of the reviewed piezoelectric actuators.

So far, the existing piezoelectric actuators are all stepping types. They are all driven step by step and there are pauses during their long range motions. This study presents a novel piezoelectric rotary motor which can output long range continuous rotary motion. With the help of two piezo-stacks which are located at a  $90^\circ$  included angle, the proposed motor can achieve circular motion trajectory of a cylindrical driving surface and the rotor can be driven by the cylindrical surface to deliver long range continuous rotary motion without pause. A series of experiments are carried out to investigate the performance of the motor prototype.

## 2. Structure and operational principle

### 2.1. Structure of the motor

The proposed piezoelectric rotary motor with specific dimensions of  $90 \times 70 \times 13.5 \text{ mm}^3$  is shown in Fig. 1. It is mainly made up of a base, a stator, a rotor, two piezo-stacks, two adjusting bolts and two shims. Two piezo-stacks preloaded by the adjusting bolts are embedded in the stator which is a metal elastic body. As the key component of the motor, the stator illustrated in Fig. 2 consists of a fixed part, a deformed part and two piezo-stack installing grooves which are located at a  $90^\circ$  included angle. The deformed part of the stator is connected to the fixed part by four flexure hinges which are designed to be quarter arcs. There is a through, round hole to assemble the rotor in the positive center of the deformed part. The cylindrical surface of the hole is well designed and processed which is utilized to driving the rotor. Besides preloading the piezo-stacks, two adjusting bolts are also used to adjust the position of the deformed part to ensure the driving surface is in an appropriate position relative to the rotor. Moreover, in order to obtain good elastic properties of the flexure hinges, the material of the stator is selected to be 65 Mn.

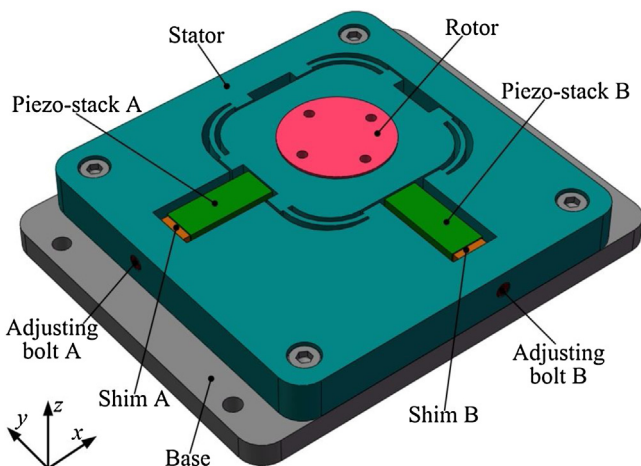


**Fig. 1.** Model of the motor.

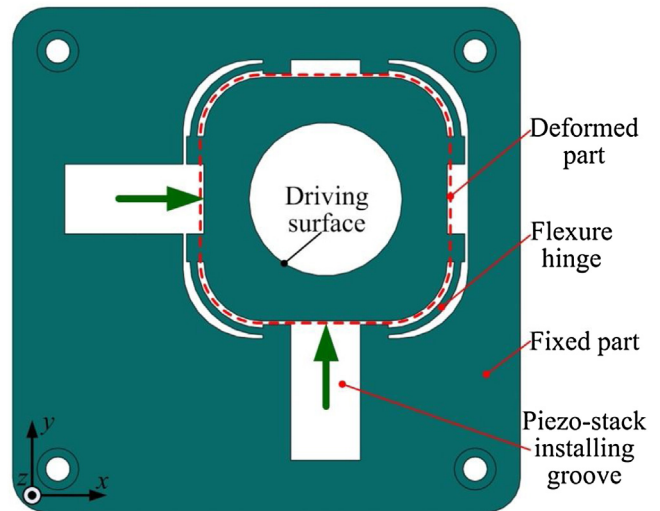


**Fig. 2.** Structure of the stator.

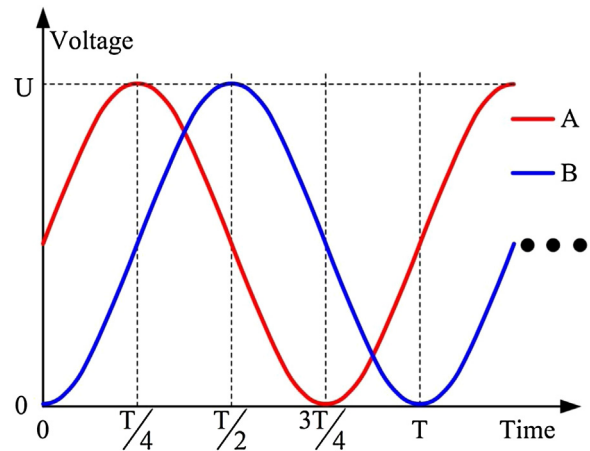


**Fig. 3.** Input signal voltages.

### 2.2. Operational principle

As Fig. 1 shows, the two piezo-stacks are assembled in installing grooves of the stator, namely piezo-stack A and piezo-stack B. When driving voltage is applied to the piezo-stack A, the deformed part of the stator is driven to generate a horizontal displacement of the driving surface in the  $x$ -direction by the extension of the piezo-stacks A. When driving voltage is applied to the piezo-stack B, the deformed part of the stator is driven to generate a vertical displacement of the driving surface in the  $y$ -direction by the extension of the piezo-stack B. So if the sine voltages with phase difference of  $90^\circ$  illustrated in Fig. 3 are applied to the piezo-stacks A and B, the deformed part of the stator is driven to generate a circular motion trajectory of the driving surface by the extensions of the two piezo-stacks and the motion trajectory of the driving surface is shown in Fig. 4.

Fig. 5 presents the operational principle of the proposed motor in a working cycle, described as follows:

- (1) As Fig. 5(A) shows, at time 0, a positive voltage  $U/2$  is applied to piezo-stack A to stretch it and the piezo-stack B is not deformed by applying zero voltage to it. So the displacement inputs A and B are  $L/2$  and 0 respectively. The driving surface is located on the bottom of the motion trajectory and the top of the driving surface contacts with the rotor.

Download English Version:

<https://daneshyari.com/en/article/5008070>

Download Persian Version:

<https://daneshyari.com/article/5008070>

[Daneshyari.com](https://daneshyari.com)